



Segmentation and genome annotation algorithms

Maxwell W. Libbrecht (0000-0003-2502-0262)¹^{*},
Rachel C.W. Chan (0000-0003-1009-6379)^{2,3}^{*},
Michael M. Hoffman (0000-0002-4517-1562)^{2,3,4,5}^{*}

1 School of Computing Science, Simon Fraser University, Burnaby, BC, Canada

2 Department of Computer Science, University of Toronto, Toronto, ON, Canada

3 Princess Margaret Cancer Centre, Toronto, ON, Canada

4 Department of Medical Biophysics, University of Toronto, Toronto, ON, Canada

5 Vector Institute for Artificial Intelligence, Toronto, ON, Canada

 These authors contributed equally to this work.

* maxwell.libbrecht@sfu.ca, michael.hoffman@utoronto.ca

Abstract

Segmentation and genome annotation (SAGA) algorithms are widely used to understand genome activity and gene regulation. These algorithms take as input epigenomic datasets, such as chromatin immunoprecipitation-sequencing (ChIP-seq) measurements of histone modifications or transcription factor binding. They partition the genome and assign a label to each segment such that positions with the same label exhibit similar patterns of input data. SAGA algorithms discover categories of activity such as promoters, enhancers, or parts of genes without prior knowledge of known genomic elements. In this sense, they generally act in an unsupervised fashion like clustering algorithms, but with the additional simultaneous function of segmenting the genome. Here, we review the common methodological framework that underlies these methods, review variants of and improvements upon this basic framework, catalogue existing large-scale reference annotations, and discuss the outlook for future work.

Background and motivation

High-throughput sequencing technology has enabled numerous techniques for genome-scale measurement of chemical and physical properties of chromatin and associated molecules in individual cell types. Using sequencing assays, the Encyclopedia of DNA Elements (ENCODE) Project, the Roadmap Epigenomics Project, and myriad individual researchers have generated thousands of such datasets. These datasets quantify various facets of gene regulation such as genome-wide transcription-factor binding, histone modifications, open chromatin, and RNA transcription. Each dataset measures a particular activity at billions of positions, and the collection of datasets does so in hundreds of samples across a variety of species and tissues. Transforming these quantifications of diverse properties into a holistic understanding of each part of the genome requires effective means for summarization. Segmentation and genome annotation (SAGA) algorithms (Box 1) have emerged as the predominant way to summarize activity at each position of the genome, distilling complex data into an interpretable précis of genomic activity.

SAGA algorithms take as input a collection of genomic datasets, such as ChIP-seq measurements of histone modifications or of transcription factor binding (Figure 1).

Box 1: Terminology

SAGA. We define a segmentation and genome annotation (SAGA) algorithm as a procedure that:

1. assigns to each position of a whole genome a label (“genome annotation”),
2. from a set of multiple (≥ 3) classes,
3. by
 - (a) integrating multiple independent observations at each position, and
 - (b) modeling dependence between adjacent positions (“segmentation”).

Previously, researchers have used several other terms to describe this task, including “segmentation” [1], “chromatin state annotation” [2] and “semi-automated genome annotation” [3].

Assay. An experiment that produces a measurement at each genomic position, such chromatin immunoprecipitation-sequencing (ChIP-seq) or assay for transposase-accessible chromatin-sequencing (ATAC-seq).

Label. One of a finite set of classes assigned to each genomic segment that shares similar activity. Other terms include “state” or “chromatin state”.

Sample. A population of cells on which one can perform an assay, such as a primary tissue sample or a cell line. Other terms include “cell type”, “epigenome”, or “biosample”.

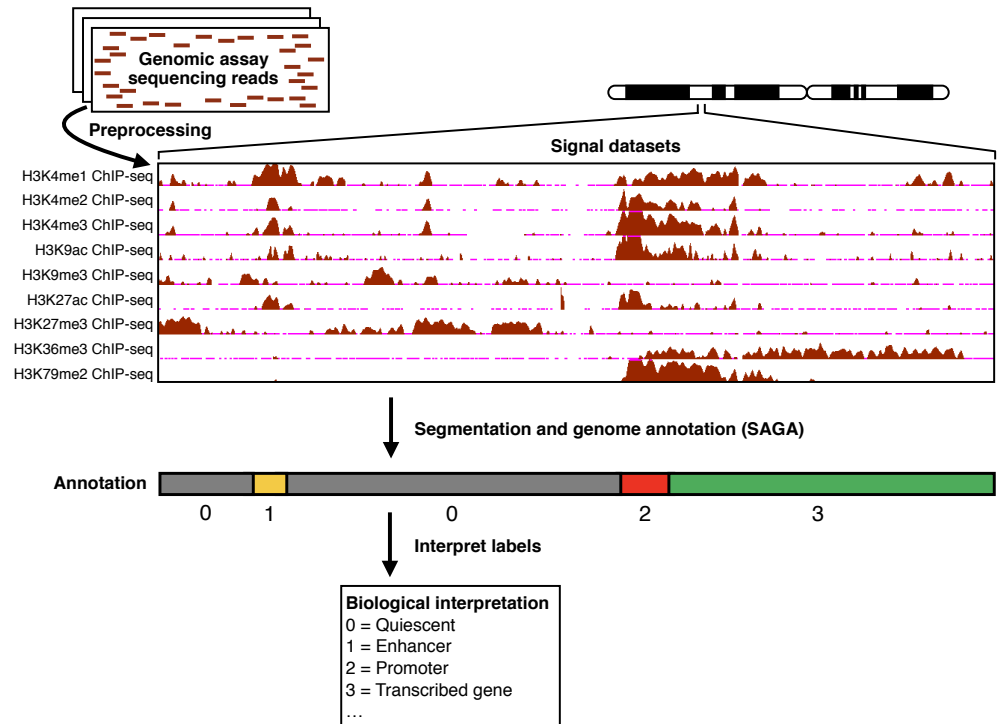


Fig 1. Overview of segmentation and genome annotation (SAGA). First, preprocessing transforms genomic assay sequencing reads into signal datasets. Second, with signal datasets as input, a SAGA algorithm partitions the genome and assigns an integer label to each segment, yielding an annotation. Third, a researcher interprets the labels, assigning a biological interpretation to each.

The SAGA task is to use the input datasets to partition the genome into segments and assign a label to each segment. SAGA algorithms perform this task in a way that leads to positions with the same label having similar patterns in the input data.

Year	Name or description	References
2007	• HMMSeg	[1]
2010	• Chromatin colors	[4]
2010	• Chromatin states model	[5]
2012	• ChromHMM	[2, 6–8]
2012	• Segway	[6, 9–11]
2013	• TreeHMM	[12]
2015	• Spectacle	[13]
2015	• hiHMM	[14]
2015	• Ensembl Regulatory Build (with Segway, ChromHMM)	[15]
2015	• EpiCseg	[16]
2015	• Segway+GBR	[3, 17]
2016	• IDEAS	[18, 19]
2017	• GenoSTAN	[20]
2017	• diHMM	[21]
2018	• iSeg	[22]
2018	• StatePaintR	[23]
2019	• RT States	[24]
2019	• ConsHMM	[25]
2020	• modHMM	[26]
2020	• SPIN	[27]
2020	• SegRNA	[28]

Table 1. Timeline of selected SAGA methods.

The first SAGA methods were developed in the 2000s, but have increased in usage recently, thanks to the wide availability of genomic datasets (Table 1). Large-scale genomic profiling projects such as ENCODE [29] and Roadmap Epigenomics [7] produced SAGA annotations as a primary output. Researchers have developed a large variety of SAGA strategies with the goal of improving upon the basic SAGA framework.

In this review, we summarize the main strategies used by most SAGA methods. Then, we discuss differences between methods, the challenges they face, and the outlook for future work.

Input data

Experimental assays used for input data

SAGA methods typically use as input a number of different experimental datasets, each describing some local property of the genome [30]. Such properties might include chromatin accessibility or presence of some DNA-binding protein. Although input data initially came from microarray methods such as tiling arrays [31], they now usually come from sequence census assays [32].

A standard collection of input datasets might measure histone modifications or DNA-binding proteins (using assays like ChIP-seq [33] or cleavage under targets and release using nuclease (CUT&RUN) [34]), and chromatin accessibility (using assays like deoxyribonuclease-sequencing (DNase-seq) [35, 36] or ATAC-seq [37]). Supplying a SAGA algorithm with datasets that measure chromatin activity yields an output

annotation that captures the regulatory state of chromatin. Creating these chromatin activity annotations has served as the predominant use of SAGA methods thus far.

Less frequently, researchers have gone beyond measurements of chromatin and DNA-binding proteins and have used SAGA methods for other kinds of data. The output annotation summarizes the input datasets, so the choice of input greatly influences the annotation’s content and its subsequent interpretation. SAGA methods can work for any sort of dense linear signal along the genome. Individual studies have applied it DNA replication timing data [3, 24, 27], interspecies comparative genomics data [25], and RNA-seq data [28]. Other studies have even found ways to incorporate non-linear chromatin 3D genome organization data into the SAGA framework [3, 27].

Signal representation of genomic assays

Most genomic assay data so far has come from bulk samples of cells. These data depict a noisy mixture of sampling an assayed property from the many cells within the population. These cells may represent subpopulations of slightly different types, or within different cell cycle stages. Thus, each subpopulation might have different characteristics in the assayed properties. In the mixture of cell subpopulations, only frequently sampled properties will rise above background noise. By comparison, less frequently sampled properties seen in a minority of cells, may remain indistinguishable from background noise.

Often, the property examined by an epigenomic assay is exhibited or not exhibited by some position of a single chromosome in a single cell, with no gradations between the extremes. For example, at some nucleotide of one chromosome in a single cell, an interrogated histone modification is either present or it is not. A single diploid cell has two copies of the chromosome. Thus, at that position, each eudiploid cell can have only 0, 1, or 2 instances of the histone modification.

Summing or averaging discrete counts over a population of cells leads to a representation of the assay data called “signal”. Signal appears as a continuous-scale measurement. Signal arises, however, only from the aggregation of position-specific properties, which in each cell may have only a small number of potential ordinal value at the moment of observation.

Unlike epigenomic assays, transcriptomic assays can measure any number of transcript copies of one position per cell. Despite similar data representations, one must avoid the temptation to interpret epigenomic signal intensity as one might interpret transcriptomic signal intensity. For a transcriptomic assay, greater signal intensity for a transcriptomic assay might reflect a greater “level” of some transcriptional property within each cell. For an epigenomic assay, greater signal intensity indicates primarily that a higher number of cells within a sample have the property of interest.

In both the epigenomic and transcriptomic cases, it remains difficult or impossible to untangle the contribution to higher signal intensity that arises from frequency of molecular activity within each cell of a subpopulation from that from the composition of subpopulations within a whole bulk population. Improvements in single-cell assays, however, may enable SAGA algorithms on data from single cells in the near future (see “Outlook for future work”).

Preprocessing of input data

SAGA methods generally use a signal representation of the input data. This signal representation originates from raw experimental data, such as sequencing reads, by way of a preprocessing procedure. For simplicity, we describe the steps of preprocessing as if a human analyst conducted them all individually, although some SAGA software packages might perform some steps without manual intervention:

Required preprocessing for all SAGA methods:

1. The analyst transforms the experimental data into raw numeric signal data.
 - For sequencing data, the analyst:
 1. Aligns each sequencing read to the reference genome,
 2. May choose to extend each read to an estimated length of the DNA fragment it begins, and
 3. Computes the number of reads per base or extended reads per base for each genomic position [9, 10].
 - For microarray data, the analyst:
 1. Acquires microarray signal intensity for the experimental sample and for a control sample, and
 2. Computes the ratio of experimental intensity to control intensity.
2. The analyst chooses units to represent the strength of activity at each position and may perform further transformation of the raw numeric signal data into these units.
 - For sequencing data, the analyst commonly uses one of:
 - Read count (no transformation),
 - Fold enrichment of observed data relative to a control [6], or
 - $-\log_{10}$ Poisson p-values indicating the likelihood of statistically significant peaks relative to control [19].The latter two units can mitigate experimental artifacts because they compare to a control experiment such as a ChIP input control.
 - For microarray data, the analyst commonly performs \log_2 transformation of the intensity ratios [4, 38, 39].

Optional preprocessing or preprocessing required only for specific SAGA methods:

3. The analyst may normalize data to harmonize signal across cell types [40]. Normalization proves especially important when annotating multiple cell types (see “Annotating multiple cell types”).
4. To prevent large outlier signal values from dominating the results, the analyst may transform signals using one of three variance-stabilizing transformations of each signal value x :
 - $\operatorname{asinh} x$ [9],
 - $\log_2(x + \text{pseudocount})$ [19], or
 - an empirical variance-stabilizing transformation [41].
5. The analyst may downsample 1-bp resolution signal into bins (see “Spatial resolution”). This involves computing one of:
 - Average read count,
 - Reads per million mapped reads fold enrichment [42],
 - Total count of reads [16, 43, 44], or
 - Maximum count of reads of each bin [6, 18].Binning greatly decreases the computational cost of the SAGA algorithm and can improve the data’s statistical properties.
6. The analyst may binarize numeric signal data into presence/absence values [2, 12, 21, 45, 46]. Binarizing signal simplifies analysis by avoiding issues related to the choice of units, but eliminates all but 1 bit of information about signal intensity per bin.

Missing data

Genomic assays almost always cannot produce signal for every region of the whole genome. Regions where an assay cannot provide reliable information about the interrogated property constitute “missing data” for that assay. Missing data in sequencing assays may arise due to unmappable sequences, which occur when repetitive reads do not uniquely map to a region [47, 48]. Missing data in microarray assays comes from regions covered by no microarray probes. There are three main ways to treat regions of missing data: (1) by treating missing data as 0-valued data, (2) by decreasing the model resolution, averaging over available data so that the missing data has limited impact, or (3) statistical marginalization over the missing data [9, 49].

When analyzing coordinated assays across multiple cell types, researchers may have to contend with having no data on some properties within a subset of cell types. This represents another kind of missing data: one with an entire dataset missing rather than only data at specific positions. Researchers can impute [21] entire missing datasets through tools such as ChromImpute [50], PREDICTD [51] or Avocado [52]. Alternatively they can use a SAGA model with built-in capability for handling the missing datasets [12].

Hidden Markov model (HMM) formulation

Many SAGA methods rely on an HMM, a probabilistic model of the relationships between sequences of observed events and the unobservable hidden states which generate the observed events. The structure of HMMs, and similar models such as dynamic Bayesian networks (DBNs) [53], naturally reflect the SAGA task of clustering observed data generated by processes that act on sequences of genomic positions.

Simple HMM example

As an illustration of a simple HMM, consider a dog, Rover, and his owner, Thomas. Thomas is 5 years old and too short to see out of the windows in his home. Rover can leave the house through his dog door and loves taking walks, playing indoors, and napping. Every morning, he will either wait by the door for Thomas, play with his squeaky toys, or sleep in. Whichever action he takes depends on the weather he sees outdoors. For example, on rainy days Rover will more likely nap or play with his toys indoors.

Thomas must infer the state of the weather outside, hidden to him, based on the behavior he observes from Rover. Thomas knows the general weather patterns outside near his home—for example, that rainy weather likely continues across multiple days.

This scenario fits well into the an HMM framework. It has a sequence of observations (Rover’s behavior) generated by hidden, non-independent unobservables (the weather outside). One would like to infer the sequence of hidden unobservables based on the sequence of observations.

Mathematical formulation

Formally, we can define an HMM over time $t \in \{1, \dots, T\}$ as follows [54, 55]. Let the sequence of observed events $\mathbf{X} = \{X_t\}_{t=1}^T$ consist of each observed event X_t at every time t . Let the sequence of hidden states $\mathbf{Q} = \{Q_t\}_{t=1}^T$ consist of each hidden state Q_t at every time t . Each Q_t takes on a value q_t from a set of m possible hidden state values (Figure 2a).

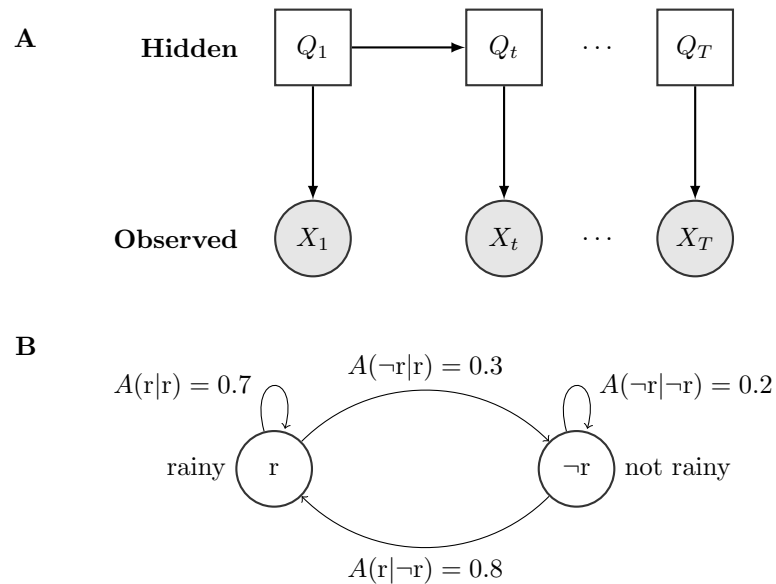


Fig 2. Two representations of an HMM. (a) Conditional dependence diagram representation of an unrolled HMM with sequence of hidden states $\{Q_t\}_{t=1}^T$ and sequence of observations $\{X_t\}_{t=1}^T$. In this representation, each node represents a hidden discrete (white rectangle) or observed continuous (grey circle) random variable. For every index t , each hidden random variable Q_t takes on some value q_t ; similarly, each observed variable X_t takes on some value x_t . X_t may represent either scalar or vector observations. Solid arcs represent conditional dependence relationships between random variables. (b) State transition diagram representation of Rover and Thomas’s weather example. In this representation, each node represents a potential value of the hidden variable Q_t . The hidden variable takes on values r (rainy) or $\neg r$ (not rainy) on any given day t . Solid arcs represent transitions between hidden states, which have transition probabilities A .

Under the Markov assumption, the probability of realizing state value q_{t+1} at the next time step $t + 1$ depends only on the current state value q_t :

$$P(Q_{t+1} = q_{t+1} | Q_t = q_t, Q_{t-1} = q_{t-1}, \dots, Q_1 = q_1) = P(Q_{t+1} = q_{t+1} | Q_t = q_t).$$

We define the transition probability $A(q_{t+1}|q_t) = P(Q_{t+1} = q_{t+1} | Q_t = q_t)$, which reflects the frequency of moving from state q_t to state q_{t+1} .

We define the emission probability $B(x_t|q_t) = P(X_t = x_t | Q_t = q_t)$ as the probability that the observable X_t is x_t if the present hidden state $Q_t = q_t$. Specifically, we assume that $B(x_t|q_t)$ depends only on $Q_t = q_t$, such that

$$P(X_t = x_t | Q_t = q_t, Q_{t-1} = q_{t-1}, \dots, Q_1 = q_1) = P(X_t = x_t | Q_t = q_t).$$

Finally, we define the hidden state probability at the first time step as $\pi_0(q_0) = P(Q_0 = q_0)$. We can fully define an HMM $M = (A, B, \pi_0)$ by specifying all of A , B and π_0 .

In the case of Rover and Thomas, we have $m = 2$ possible hidden states (rainy, not-rainy) and 3 possible observations (Rover is napping, playing indoors, or waiting by the door). To Thomas, the hidden variable Q_t captures the weather outside, while the observed variable X captures Rover's behavior. The probability of the state of the weather outside changing on a day-to-day basis is defined by the transition probabilities A (Figure 2b). The probability of Rover's behavior, given the weather, is defined by the emission probabilities B .

Algorithms for inference, decoding, and training

Inference

The main task one uses HMMs for is to quantify how well some predicted sequence of hidden states fits the observed data. Other common tasks like decoding or training serve as variations of, or build on, this inference task.

In HMMs inference, we can compute the likelihood of any sequence of hidden states \mathbf{Q} . We use the sequence of observed events \mathbf{X} and the model probabilities M to compute the likelihood function $P(\mathbf{X}|\mathbf{Q}, M)$. The likelihood function is the probability that our predicted sequence of hidden states produced our observed sequence of observed states. We often compute the likelihood function using the forward-backward algorithm [56, 57].

Viterbi decoding

Given a sequence of observed events \mathbf{X} , we often wish to know the maximum likelihood sequence of corresponding hidden states \mathbf{Q} . For example, if Thomas observes that in the past 3 mornings, Rover slept, played, and then slept again, what weather sequence outside is most likely?

To answer this question, we decode the optimal sequence of hidden states \mathbf{q}^* such that $\mathbf{q}^* = \arg \max_{\mathbf{Q}} P(\mathbf{Q}|\mathbf{X}, M)$. The Viterbi algorithm [58] provides an efficient solution for this problem, making it unnecessary to compare the likelihood for every possible sequence of hidden states.

Training

Usually, we do not know the model parameters (A, B, π_0) and must learn them from data. We define training as the process of learning these parameters, and training data as the sequence of observations upon which we learn. An efficient algorithm that finds the global optimum parameter values for some training data does not exist. Instead,

researchers commonly train HMMs using expectation-maximization (EM) [59] algorithms such as the Baum-Welch algorithm [60], which find a local optimum. Other reviews [54] describe inference and training methods in more detail.

HMMs for SAGA

We can readily apply the HMM formalization to genomic data for use in SAGA methods. Instead of time, we define the dynamic axis t in terms of physical position along a chromosome. Each position t refers to a single base pair or, in the case of lower-resolution models, a fixed-size region (see “Spatial resolution”). The observation at each genomic position usually represents genomic signal (see “Input data”). Each position’s hidden state represents its label (see “Understanding labels”). As a result, decoding the most probable sequence of hidden states reveals the most probable sequence of labels across the genome. We call this resulting sequence of labels an annotation.

Many SAGA methods use an HMM structure [2, 9, 12, 16, 21, 24, 39, 42], or generalizations thereof. For example, DBNs are generalizations of HMMs that can model connections between variables over adjacent time steps. Methods such as Segway [9] use a DBN model in their approach to the SAGA problem. This can make it easier to extend the model to tasks such as semi-supervised, instead of unsupervised, annotation [61].

Understanding labels

SAGA methods are unsupervised. The labels they produce usually begin with integer designations without any essential meaning. Ideally each label corresponds to a particular category of genomic element. To make this correspondence explicit, we must assign a biological interpretation, such as “Enhancer” or “Transcribed gene”, to each label.

Usually, one makes assignments of labels to biological interpretations in a post-processing step. In post-processing, a researcher compares each label to known biological phenomena and assigns an interpretation that matches the researcher’s understanding of molecular biology. For example, a label characterized by the histone modification H3K36me3 (associated with transcription) and enriched in annotated gene bodies might have the interpretation “Transcribed”. A label characterized by H3K27ac and H3K4me1, both histone modifications canonically associated with active enhancers, might have the interpretation “Enhancer” [29].

The interpretation process provides an opportunity to discover new categories of genomic elements. For example, one SAGA study found that their model consistently produces a label corresponding to transcription termination sites. Previously, none had described a distinctive epigenetic signature for transcription termination [6].

Manual interpretation proves time-consuming for human analysis. Applying SAGA to multiple cell types independently exacerbates this problem (see “Annotating multiple cell types”).

Two existing methods automate the label interpretation process: expert rules and machine learning. In both cases, an interpretation program considers the information that a researcher would use for interpretation. This includes examining the relationship between labels and individual input data properties. It also includes reviewing colocalization of labels with features in previously created annotations. These annotations may have come from SAGA approaches or other manual or automated methods.

In the expert rule approach, an analyst designs rules about what properties a given label must have to receive a particular interpretation. The analyst then applies these rules to assign interpretations to labels from all models [15].

In the machine learning approach, one trains a classifier on previous manual annotations. The classifier then learns a model that assigns interpretations to labels given their properties [11]. One analysis [11] found that automatic interpretation agreed with manual for 77% of labels, compared to 19% expected by chance.

Spatial resolution

Baroque music often employs a musical architecture known as “ternary form”. Specifically, pieces of this structure follow a general “ABA” pattern, whereupon the second “A” section recapitulates the first with some variation. Each section contains multiple musical “sentences”, which may repeat or vary. Just like linguistic sentences, each musical sentence contains clusters of notes, or motifs, between “breaths” in the musical articulation. Finer examination of the motifs shows they contain a few notes and chords each. Finer examination of the notes themselves shows they behave just like isolated phonemes in speech, with little meaning on their own.

The genome resembles a musical composition in that one observes different behaviors at different scales. The scale of genomic behavior one wishes to observe influences the choice of SAGA method and parameters chosen for the method. To observe nucleosome-scale behavior such as genes, promoters and enhancers, one desires $\sim 10^3$ bp segments. To describe behavior on the scale of topological domains [62], one desires segments of length 10^5 bp to 10^6 bp [1, 3, 17].

The most important parameter influencing segment length is the underlying resolution of the SAGA method. As noted above (see “Input data”), most SAGA methods downsample data into bins. To observe nucleosome-scale segment lengths ($\sim 10^3$ bp), one should use one should use 100 bp to 200 bp resolution [2, 9, 18]. To observe domain-scale segment lengths ($\sim 10^5$ bp), one should use $\sim 10^4$ bp resolution [3, 4, 27]. Segway [9] and RoboCOP [63] provide some of few SAGA methods optimized for single-base resolution inference, and can identify behavior on a 1 bp scale. While most existing SAGA methods handle data at just one genomic scale, there exist methods capable of learning from data at multiple genomic scales [21].

Limitations of of the experimental data itself influence the choice of SAGA model resolution. Spatial imprecision in ChIP-seq data gives it an inherent resolution of about 10 bp. More precise assays such as ChIP-exo [64] and ChIP-nexus [65] can approach 1 bp resolution. Conversely, assays like DNA adenine methyltransferase identification (DamID) and Repli-seq have a coarser resolution of ≥ 100 bp.

The desired scale may also influence the choice of input data. When aiming to annotate at the domain scale, one should include data with activity at this scale, such as replication time data and Hi-C data [3, 4, 24, 27]. The inclusion of long-range contact information from Hi-C data poses a challenge because standard algorithms for HMMs cannot be used for a probabilistic model that includes long-range dependencies. Therefore, one must instead use alternative approaches such as graph-based regularization [3] or approximate inference [27].

SAGA methods model segment length through their transition parameters. HMM models assume a geometric distribution in determination of a segment’s length [66]. Related DBN methods can include constraints to tune segment length further. Constraints include the enforcement of a minimum or maximum segment length [9]. Enforcement of a minimum segment length ensures that one does not obtain segments shorter than the effective resolution of the underlying data or biological phenomena. Probabilistic models often additionally use a prior distribution on the transition

parameters during training to encourage them to produce shorter or longer segment lengths.

Choosing the number of labels

Most SAGA methods require the user to define the number of labels. Using more labels increases the granularity of the resulting annotation at the cost of added complexity. Typically, the number of labels ranges from 5–20, with more recent work favoring 10–15 labels.

One might think to make the choice of number of labels automatically with a statistical approach. The Akaike information criterion (AIC), Bayes information criterion (BIC), and factorized information criterion (FIC) [67] measure the statistical support a particular number of labels has. Instead of a fixed number of labels, one may give the model flexibility to choose the number of labels during training and include a hyperparameter that encourages it to choose a higher or lower number [14]. Or one might define labels according to local minima in an optimization based on a network model of assays [46]. One could even exhaustively assign a separate label to every observed presence/absence pattern in binary data [43].

In practice, however, researchers rarely use these statistical approaches for determining the number of labels. Optimizing an information criterion does not necessarily yield the most interpretable annotation. Interpretability reigns supreme in most SAGA applications. End users find annotations most useful when they have about 5–20 labels for two reasons. First, most can only articulate that many known distinctions between classes of genomic elements. Second, even if one could find meaningful distinctions between a large number of labels, few using the resulting annotations could keep fine distinctions between such a large number of patterns in their working memory. [68] Even if a statistical approach supported the use of 50 labels, the complexity of such an annotation would make it impractical for most users.

Annotating multiple cell types

There now exist epigenomics datasets describing hundreds of biological samples (Figure 3a). Researchers have correspondingly adapted SAGA methods to work with many samples simultaneously.

We use the term “sample” to refer to some population of cells on which one can perform an epigenomic assay. A sample could correspond to a primary tissue sample, a cell line, cells affected by some perturbation such as drug or disease, or even cells from different species.

The simplest approach for annotating multiple samples involves simply training a separate model on each sample [11] (Figure 3b). The large number of models produced by this approach necessitates using an automated label interpretation process (see “Label interpretation”).

Two categories of approaches aim to share information across samples. The first, “horizontal sharing” or “concatenated” approaches, share information between samples to inform the label-training process. The second, “vertical sharing” or “stacked” approaches, share position-specific information to inform the label assignment of each position.

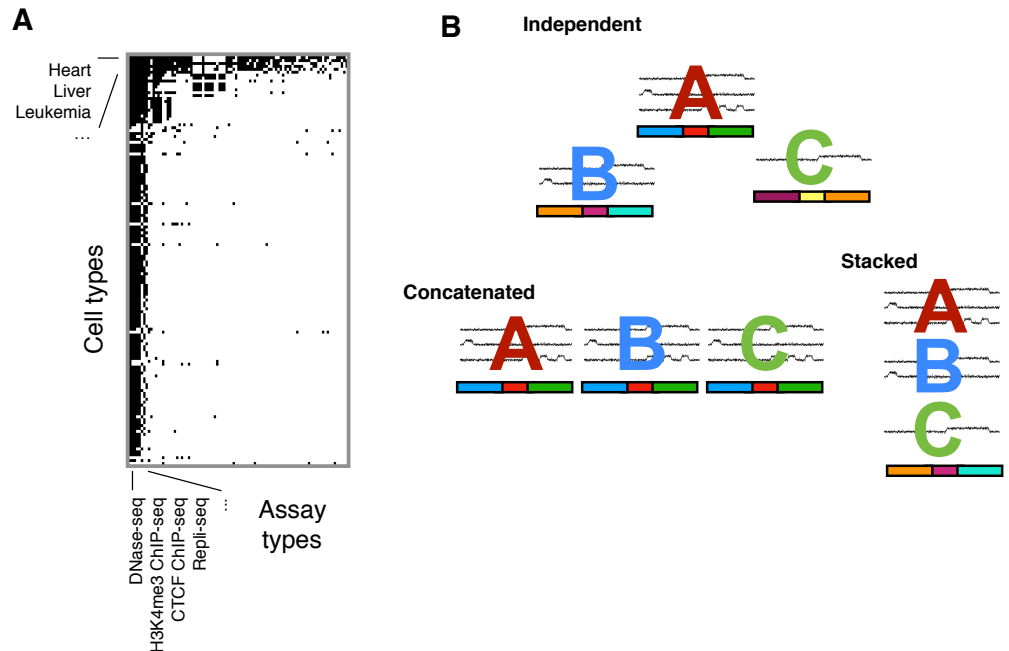


Fig 3. Annotating multiple cell types. (a) Datasets generated by the ENCODE and Roadmap Epigenomics consortia as of 2019. The black cells represent the datasets actually generated out of a larger number of potential combinations of cell type and assay type. (b) Annotating 6 datasets from 3 different samples: 3 from cell type A, 2 from cell type B, and 1 from cell type C. Colored letters over signal data indicate data associated with those samples. One can use three different SAGA strategies with this collection of datasets: *Independent*: Performing training and inference completely independently on each sample. This yields a different annotation for each sample. *Concatenated* (horizontal sharing): Training a single model across all cell types. This yields one annotation per sample with a shared label set. Each sample must have the same datasets, necessitating imputation of any missing datasets. *Stacked* (vertical sharing): Performing training and inference on datasets from all samples. This yields a single pan-cell-type annotation.

Horizontal sharing: emphasizing similarities across samples for learning labels

The simplest way to remove the need for interpreting multiple models is to apply a single model across many samples. To do this, one can treat each sample as referring to separate copies of a longer genome added horizontally after the first one in a “concatenated” approach (Figure 3b). One performs concatenated training and inference little differently than if the data from different samples pertained to different chromosomes in the same genome. Because all samples share a single concatenated model, researchers need only perform post-processing interpretation once.

The concatenated approach has wide usage [6, 7, 69], but has two downsides. First, concatenated SAGA requires that every sample has data from the same assays. In practice, this criterion often does not hold true. This means that—unless these assays are imputed or treated as missing (see “Vertical sharing: emphasizing similarities across samples in positional information”)—one must exclude data for an assay conducted in even all but one samples. In a simple concatenated approach, one cannot annotate a sample which lacks even one dataset present in the others.

Second, data from different samples can have artifactual differences or batch effects. Applying the same model across multiple cell types assumes that all datasets from the same assay type have similar statistical properties. This can result in label distributions to vary wildly across samples and biologically implausible sample-specific labels. Data normalization can help abate the problem of different statistical properties between samples, but usually does so incompletely. This problem is particularly significant when using continuous signal. In contrast, binarizing the data (see “Input data”) can cover up some experimental biases.

One might expect that concatenated annotation would benefit training by increasing the amount of training data. As it turns out, multiplying the amount of training data does not significantly aid the training process, as the types of labels vary little across samples. Most complex eukaryotic organisms studied with SAGA have very large genomes, and just one sample provides plenty of training data. In fact, for computational efficiency, researchers often train on just a fraction of the available samples [7], a fraction of the genome from a given sample [9] or both.

Vertical sharing: emphasizing similarities across samples in positional information

Another class of multi-sample SAGA methods shares position-specific information across samples as part of the annotation process. These methods take advantage of the non-independence of biological activity across samples at a genomic position. For example, if a given position has an active enhancer label in many samples, it is more likely to act as an active enhancer in a new sample.

The simplest type of vertical sharing approach learns a model on data from all samples jointly (Figure 3b). One can implement this “stacked” approach by adding datasets from all samples vertically into a single combined model. A stacked model captures patterns of activity across multiple cell types. For example, a stacked model, unlike an independent model, can find a label for an enhancer active in cell type A and cell type B but inactive in cell type C.

Although conceptually simple, the stacked approach tends not to work well for more than several cell types. Stacking fails with larger number of cell types because each pattern of activity requires its own label. Therefore, the number of labels must grow exponentially in the number of samples. A simple stacked model that treats all assays as independent also ignores the relationship between assays on the same cell type, or the same assay type on different cell types.

A second approach uses a concatenated model that additionally learns a position-specific preference over the labels for each position. Through this preference, data from one sample can influence inference on another. Two implementations have applied variants of this hybrid horizontal-vertical sharing approach. First, TreeHMM [12] uses a cellular lineage tree as part of its input. For each genomic position, TreeHMM models statistical dependency between the label of a parent cell type and that of a child cell type. Second, IDEAS [18] uses a similar approach to TreeHMM, but dynamically identifies groups of related samples rather than using a fixed developmental structure. The IDEAS model allows these sample groups to vary across positions, which allows for different relationships between samples in different genomic regions.

A third approach for vertical sharing uses a pairwise prior to transfer position-specific information between cell types [3, 17]. In other words, if position i and position j received the same label in many other samples, then they should be more likely to receive the same label in an additional sample. In contrast to the other methods in this section, the pairwise prior approach does not require the use of concatenated annotation. Therefore, the pairwise approach has the advantage of not requiring the same available data in all cell types.

A fourth approach imputes missing datasets in the target cell type, then applies any of the above annotation methods to the imputed data [50]. Imputation provides three advantages. First, it ensures that all target cell types have the same set of datasets. Second, one can conduct imputation entirely as a preprocessing step, allowing the use of any SAGA method afterward. Third, the imputation process can normalize some artifactual differences between datasets, making concatenated annotation more appropriate.

Vertical sharing approaches have the downside that one cannot understand the annotation of each sample in isolation. This arises from the influence on label assignments in one sample by data from other samples. In particular, vertical sharing tends to mask differences between samples. For example, if some position has an enhancer label in many samples, vertical sharing approaches will annotate that position as an enhancer in a target cell type too, even with no enhancer-related data in the target cell type.

Using and visualizing SAGA annotations

Name	Method	Labels	Samples	Datasets per sample	Reference
Roadmap (5 mark)	ChromHMM concatenated	15	127	5	[7]
Roadmap (6 mark)	ChromHMM concatenated	18	98	6	[7]
Roadmap (imputed)	Impute+ChromHMM	25	127	5–12	[7]
IDEAS	IDEAS	20	127	5	[19]
Segway Encyclopedia	Segway independent	14–33	164	3–126	[11]
Segway domains	Segway+GBR	5	8	12	[3]
Ensembl Regulatory Build	ChromHMM independent	25	89	6–10	[15]

Table 2. Existing large-scale human reference annotations.

A number of resources can aid in the application of SAGA algorithms and annotations. Reference annotations exist for many cell types (Table 2). These obviate the need for a user of the annotation to actually run a SAGA method. Alternatively, if the user must run a SAGA algorithm on their own data, standardized protocols describe how to perform this process [8, 70].

Most users of SAGA annotations view them through one of three visualization strategies. The first, and most common, strategy displays individual annotations as

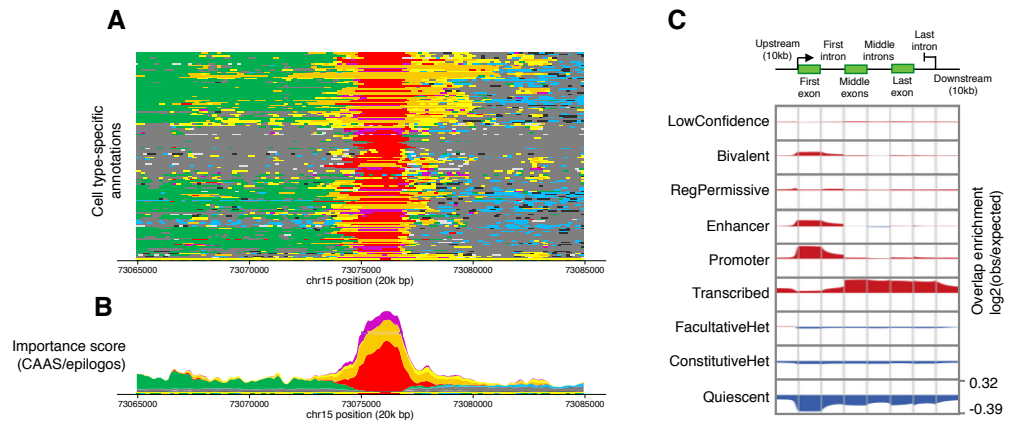


Fig 4. Visualizations of SAGA annotations. (a) Genome browser display showing 164 cell type annotations for a 20 kbp region on human chromosome 15 (GRCh37/hg19) [71]. Each annotation has 8 labels: Promoter (red), Enhancer (orange), Transcribed (green), Permissive regulatory (yellow), Bivalent (purple), Facultative heterochromatin (light blue), Constitutive heterochromatin (black), Quiescent (grey), and Low Confidence (light grey). (b) Importance score (conservation-associated activity score (CAAS)) for the same region. Total height at each position indicates the position's estimated importance. Height of a given color band denotes the contribution towards importance of the associated label. (c) Genome-wide visualization of the SAGA annotation for 164 samples aggregated over GENCODE [72] protein-coding gene components. Rows: the 9 labels of the annotation. Columns: gene components, including 10 kbp flanking regions upstream and downstream. Each cell shows the enrichment of the row's label with a position along the column's component. Figures derived from [11].

individual rows or “tracks” on a genome browser (Figure 4a). In each row, the browser displays the segments of that annotation for a region of one chromosome, usually indicating the label by color. Popular genome browsers for displaying segmentations include the University of California, Santa Cruz (UCSC) Genome Browser [73], the Washington University in St. Louis (WashU) Epigenome Browser [74], and Ensembl [75].

A second visualization strategy integrates annotations of all samples (Figure 4b). This visualization stacks all labels for a given position on top of one another and scales the vertical axis by an estimate of functional importance of that position. Two methods can estimate this importance: Epilogos (<https://epilogos.altius.org/>), which emphasizes rare activity, and the CAAS, which measures activity that is correlated with evolutionary conservation [11].

A third visualization strategy aggregates information about each label across the entire genome. This shows the enrichment of each label at positions of known significance, such as gene components (Figure 4c) or curated enhancers. Tools such as Segtools [76] and deepTools [77] can create these visualizations.

SAGA annotations can provide valuable reference datasets to other analyses and tools. The assignment of one and only one label from a small set to every mappable part of the genome greatly eases downstream analyses. SAGA annotations summarize genomic activity in a much simpler way than the individual input datasets, and even than processed versions of the input datasets such as peak calls.

Most SAGA annotations are in the tab-delimited browser extensible data (BED) format (<https://genome.ucsc.edu/FAQ/FAQformat.html#format1>). This makes it easy to remix SAGA annotations with other datasets using powerful software such as BEDTools [78]. SAGA annotations form building blocks for methods for integrative analysis of genomic data such as CADD [79].

Conclusions and outlook for future work

SAGA methods provide a powerful and flexible tool for analyzing genomic datasets. These methods promise to continue to play an important role as researchers generate more datasets. Despite the large existing literature, future work could still address many challenges.

Alternate scales and data types. Nucleosome-scale annotations (100 bp to 1000 bp segments) of histone modifications have wide usage. While annotations of different data types or at different length scales exist, they are less widely used. Currently, there exist reference domain annotations with segments of length 10^5 bp to 10^6 bp for only a small number of samples [3, 4, 42, 80], and few or no annotations at other scales.

Data preprocessing . Genome annotations would improve with better processing and normalization of input datasets. Representations such as fold enrichment used by existing methods seem primitive compared to more rigorous quantification schemes used in RNA-seq analysis such as transcripts per million (TPM). One could also improve SAGA preprocessing by more frequently incorporating information from multi-mapping reads [81].

Confidence estimates. Most methods do not report any measure of confidence in their predictions. Two types of confidence would prove useful. First, one would often like to know the level of confidence that a position in some sample has label X and not label Y. Second, in many cases one would like to have confidence in a differential labeling between two samples—that cell type A and cell type B have different labels.

Two methods work towards a solution for the second problem [82, 83], but there remains much room for further work.

Continuous representations. Existing SAGA methods output a discrete annotation, assigning a single label to each position. In this discrete approach, annotations cannot easily represent varying strength in activity of genomic elements or elements that simultaneously multiple types of activity. A continuous annotation approach analogous to the topic models used for text document classification might address this limitation [84].

Single cell data. Existing SAGA methods use data from bulk samples of cells. Increasing availability of data from single-cell assays necessitates the development of methods that can leverage this additional information.

Pan-cell-type annotation. The semantics of genome annotations correspond poorly to the way most molecular biologists conceptualize genomic elements. Most existing annotations are cell-type-specific—the annotation states that a given locus acts as an active enhancer in cell type A. In contrast, researchers often state that a given locus “is an enhancer”.

In contrast, other annotations—such of those of protein-coding genes—serve as a pan-cell-type characterization. Each gene has a fixed location, and only its expression varies across samples.

There exists a need for pan-cell-type epigenome annotations. Such an annotation would define fixed intervals for regulatory elements such as promoters, enhancers, and insulators, and it would specify in which samples each element is active. Specifically targeting this task in the SAGA model could improve results over pan-cell-type annotations assembled from multiple cell-type-specific SAGA models [11].

Author contributions

Conceptualization, M.W.L. and M.M.H.; Funding acquisition, M.M.H.; Investigation, M.W.L., R.C.W.C., and M.M.H.; Visualization, M.W.L. and R.C.W.C.; Writing — original draft, M.W.L., R.C.W.C., and M.M.H.; Writing — review & editing, M.W.L. and M.M.H.

Acknowledgments

This work was supported by the Natural Sciences and Engineering Research Council of Canada (RGPIN-2015-03948 to M.M.H.)

Competing interests

The authors declare no competing interests.

Acronyms

AIC Akaike information criterion

ATAC-seq assay for transposase-accessible chromatin-sequencing

BED browser extensible data
BIC Bayes information criterion
CAAS conservation-associated activity score
ChIP-seq chromatin immunoprecipitation-sequencing
CUT&RUN cleavage under targets and release using nuclease
DamID DNA adenine methyltransferase identification
DNase-seq deoxyribonuclease-sequencing
DBN dynamic Bayesian network
EM expectation-maximization
ENCODE Encyclopedia of DNA Elements
FIC factorized information criterion
HMM hidden Markov model
SAGA segmentation and genome annotation
TPM transcripts per million
UCSC University of California, Santa Cruz
WashU Washington University in St. Louis

References

1. Day N, Hemmaplardh A, Thurman RE, Stamatoyannopoulos JA, Noble WS. Unsupervised segmentation of continuous genomic data. *Bioinformatics*. 2007;23(11):1424–1426.
2. Ernst J, Kellis M. ChromHMM: automating chromatin-state discovery and characterization. *Nature Methods*. 2012;9(3):215–216.
3. Libbrecht MW, Ay F, Hoffman MM, Gilbert DM, Bilmes JA, Noble WS. Joint annotation of chromatin state and chromatin conformation reveals relationships among domain types and identifies domains of cell-type-specific expression. *Genome Research*. 2015;25(4):544–557.
4. Filion GJ, van Bommel JG, Braunschweig U, Talhout W, Kind J, Ward LD, et al. Systematic protein location mapping reveals five principal chromatin types in *Drosophila* cells. *Cell*. 2010;143(2):212–224.
5. Ernst J, Kellis M. Discovery and characterization of chromatin states for systematic annotation of the human genome. *Nature Biotechnology*. 2010;28(8):817–825.
6. Hoffman MM, Ernst J, Wilder SP, Kundaje A, Harris RS, Libbrecht M, et al. Integrative annotation of chromatin elements from ENCODE data. *Nucleic Acids Research*. 2012;41(2):827–841.

7. Kundaje A, Meuleman W, Ernst J, Bilenky M, Yen A, Heravi-Moussavi A, et al. Integrative analysis of 111 reference human epigenomes. *Nature*. 2015;518(7539):317–330.
8. Ernst J, Kellis M. Chromatin-state discovery and genome annotation with ChromHMM. *Nature Protocols*. 2017;12(12):2478–2492.
9. Hoffman MM, Buske OJ, Wang J, Weng Z, Bilmes JA, Noble WS. Unsupervised pattern discovery in human chromatin structure through genomic segmentation. *Nature Methods*. 2012;9(5):473–476.
10. Chan RC, Libbrecht MW, Roberts EG, Bilmes JA, Noble WS, Hoffman MM. Segway 2.0: Gaussian mixture models and minibatch training. *Bioinformatics*. 2018;34(4):669–671.
11. Libbrecht MW, Rodriguez OL, Weng Z, Bilmes JA, Hoffman MM, Noble WS. A unified encyclopedia of human functional DNA elements through fully automated annotation of 164 human cell types. *Genome Biology*. 2019;20(1):180.
12. Biesinger J, Wang Y, Xie X. Discovering and mapping chromatin states using a tree hidden Markov model. *BMC Bioinformatics*. 2013;14(Suppl 5):S4.
13. Song J, Chen KC. Spectacle: fast chromatin state annotation using spectral learning. *Genome Biology*. 2015;16(1):33.
14. Sohn KA, Ho JW, Djordjevic D, Jeong Hh, Park PJ, Kim JH. hiHMM: Bayesian non-parametric joint inference of chromatin state maps. *Bioinformatics*. 2015;31(13):2066–2074.
15. Zerbino DR, Wilder SP, Johnson N, Juettemann T, Flicek PR. The Ensembl regulatory build. *Genome Biology*. 2015;16(1):56.
16. Mammana A, Chung HR. Chromatin segmentation based on a probabilistic model for read counts explains a large portion of the epigenome. *Genome Biology*. 2015;16(1):151.
17. Libbrecht MW, Hoffman MM, Bilmes JA, Noble WS. Entropic graph-based posterior regularization. In: *Proceedings of the International Conference on Machine Learning*; 2015. p. 1992–2000.
18. Zhang Y, An L, Yue F, Hardison RC. Jointly characterizing epigenetic dynamics across multiple human cell types. *Nucleic Acids Research*. 2016;44(14):6721–6731.
19. Zhang Y, Hardison RC. Accurate and reproducible functional maps in 127 human cell types via 2D genome segmentation. *Nucleic Acids Research*. 2017;45(17):9823–9836.
20. Zacher B, Michel M, Schwalb B, Cramer P, Tresch A, Gagneur J. Accurate promoter and enhancer identification in 127 ENCODE and roadmap epigenomics cell types and tissues by GenoSTAN. *PLoS One*. 2017;12(1):e0169249.
21. Marco E, Meuleman W, Huang J, Glass K, Pinello L, Wang J, et al. Multi-scale chromatin state annotation using a hierarchical hidden Markov model. *Nature Communications*. 2017;8:15011.
22. Girimurugan SB, Liu Y, Lung PY, Vera DL, Dennis JH, Bass HW, et al. iSeg: an efficient algorithm for segmentation of genomic and epigenomic data. *BMC Bioinformatics*. 2018;19(1):131.

23. Coetzee SG, Ramjan Z, Dinh HQ, Berman BP, Hazelett DJ. StateHub-StatePaintR: rapid and reproducible chromatin state evaluation for custom genome annotation. *F1000Research*. 2020;7(214):214.
24. Poulet A, Li B, Dubos T, Rivera-Mulia JC, Gilbert DM, Qin ZS. RT States: systematic annotation of the human genome using cell type-specific replication timing programs. *Bioinformatics*. 2019;35(13):2167–2176.
25. Arneson A, Ernst J. Systematic discovery of conservation states for single-nucleotide annotation of the human genome. *Communications Biology*. 2019;2(1):248.
26. Benner P, Vingron M. ModHMM: A modular supra-Bayesian genome segmentation method. *Journal of Computational Biology*. 2020;27(4):442–457.
27. Wang Y, Zhang Y, Zhang R, van Schaik T, Zhang L, Sasaki T, et al. SPIN reveals genome-wide landscape of nuclear compartmentalization. *bioRxiv*. 2020;2020.03.09.982967.
28. Mendez M, FANTOM Consortium Main Contributors, Scott MS, Hoffman MM. Unsupervised analysis of multi-experiment transcriptomic patterns with SegRNA identifies unannotated transcripts. *bioRxiv*. 2020;2020.07.28.225193.
29. ENCODE Project Consortium. An integrated encyclopedia of DNA elements in the human genome. *Nature*. 2012;489(7414):57–74.
30. Zitnik M, Nguyen F, Wang B, Leskovec J, Goldenberg A, Hoffman MM. Machine learning for integrating data in biology and medicine: Principles, practice, and opportunities. *Information Fusion*. 2019;50:71–91.
31. ENCODE Project Consortium, et al. Identification and analysis of functional elements in 1% of the human genome by the ENCODE pilot project. *Nature*. 2007;447(7146):799–816.
32. Wold B, Myers RM. Sequence census methods for functional genomics. *Nature Methods*. 2007;5(1):19–21.
33. Barski A, Cuddapah S, Cui K, Roh TY, Schones DE, Wang Z, et al. High-resolution profiling of histone methylations in the human genome. *Cell*. 2007;129(4):823–837.
34. Skene PJ, Henikoff S. An efficient targeted nuclease strategy for high-resolution mapping of DNA binding sites. *eLife*. 2017;6:e21856.
35. Boyle AP, Davis S, Shulha HP, Meltzer P, Margulies EH, Weng Z, et al. High-resolution mapping and characterization of open chromatin across the genome. *Cell*. 2008;132(2):311–322.
36. Hesselberth JR, Chen X, Zhang Z, Sabo PJ, Sandstrom R, Reynolds AP, et al. Global mapping of protein-DNA interactions in vivo by digital genomic footprinting. *Nature Methods*. 2009;6(4):283–289.
37. Buenrostro JD, Giresi PG, Zaba LC, Chang HY, Greenleaf WJ. Transposition of native chromatin for fast and sensitive epigenomic profiling of open chromatin, DNA-binding proteins and nucleosome position. *Nature Methods*. 2013;10(12):1213–1218.

38. Schuettengruber B, Ganapathi M, Leblanc B, Portoso M, Jaschek R, Tolhuis B, et al. Functional anatomy of polycomb and trithorax chromatin landscapes in *Drosophila* embryos. *PLoS Biology*. 2009;7(1):e1000013.
39. Kharchenko PV, Alekseyenko AA, Schwartz YB, Minoda A, Riddle NC, Ernst J, et al. Comprehensive analysis of the chromatin landscape in *Drosophila melanogaster*. *Nature*. 2011;471(7339):480–485.
40. Xiang G, Keller CA, Giardine B, An L, Li Q, Zhang Y, et al. S3norm: simultaneous normalization of sequencing depth and signal-to-noise ratio in epigenomic data. *Nucleic Acids Research*. 2020;48(8):e43.
41. Bayat F, Libbrecht M. Variance-stabilized units for sequencing-based genomic signals. *bioRxiv*. 2020;2020.01.31.929174.
42. Larson JL, Huttenhower C, Quackenbush J, Yuan GC. A tiered hidden Markov model characterizes multi-scale chromatin states. *Genomics*. 2013;102(1):1–7.
43. Taudt A, Nguyen MA, Heinig M, Johannes F, Colome-Tatche M. chromstaR: Tracking combinatorial chromatin state dynamics in space and time. *bioRxiv*. 2016;038612.
44. Zehnder T, Benner P, Vingron M. Predicting enhancers in mammalian genomes using supervised hidden Markov models. *BMC Bioinformatics*. 2019;20(1):157.
45. Hamada M, Ono Y, Fujimaki R, Asai K. Learning chromatin states with factorized information criteria. *Bioinformatics*. 2015;31(15):2426–2433.
46. Zhou J, Troyanskaya OG. Probabilistic modelling of chromatin code landscape reveals functional diversity of enhancer-like chromatin states. *Nature Communications*. 2016;7:10528.
47. Derrien T, Estellé J, Sola SM, Knowles DG, Raineri E, Guigó R, et al. Fast computation and applications of genome mappability. *PLoS One*. 2012;7(1):e30377.
48. Karimzadeh M, Ernst C, Kundaje A, Hoffman MM. Umap and Bismap: quantifying genome and methylome mappability. *Nucleic Acids Research*. 2018;46(20):e120.
49. Lian H, Thompson WA, Thurman R, Stamatoyannopoulos JA, Noble WS, Lawrence CE. Automated mapping of large-scale chromatin structure in ENCODE. *Bioinformatics*. 2008;24(17):1911–1916.
50. Ernst J, Kellis M. Large-scale imputation of epigenomic datasets for systematic annotation of diverse human tissues. *Nature Biotechnology*. 2015;33(4):364–376.
51. Durham TJ, Libbrecht MW, Howbert JJ, Bilmes J, Noble WS. PREDICTD parallel epigenomics data imputation with cloud-based tensor decomposition. *Nature Communications*. 2018;9(1):1402.
52. Schreiber J, Durham T, Bilmes J, Noble WS. Avocado: a multi-scale deep tensor factorization method learns a latent representation of the human epigenome. *Genome Biol*. 2020;21(1):81.
53. Dean T, Kanazawa K. A model for reasoning about persistence and causation. *Computational Intelligence*. 1989;5(2):142–150.

54. Bilmes JA. What HMMs can do. *IEICE Transactions on Information and Systems*. 2006;89(3):869–891.
55. Yoon BJ. Hidden Markov models and their applications in biological sequence analysis. *Current Genomics*. 2009;10(6):402–415.
56. Ferguson JD. Variable duration models for speech. *Proceedings of Symposium on the Application of Hidden Markov Models to Text and Speech*. 1980; p. 143–179.
57. Levinson SE. Continuously variable duration hidden Markov models for automatic speech recognition. *Computer Speech & Language*. 1986;1(1):29–45.
58. Viterbi A. Error bounds for convolutional codes and an asymptotically optimum decoding algorithm. *IEEE Transactions on Information Theory*. 1967;13(2):260–269.
59. Dempster AP, Laird NM, Rubin DB. Maximum likelihood from incomplete data via the EM algorithm. *Journal of the Royal Statistical Society: Series B (Methodological)*. 1977;39(1):1–22.
60. Baum LE, Petrie T, Soules G, Weiss N. A maximization technique occurring in the statistical analysis of probabilistic functions of Markov chains. *Annals of Mathematical Statistics*. 1970;41(1):164–171.
61. Chan RC, McNeil M, Roberts EG, Mendez M, Libbrecht MW, Hoffman MM. Semi-supervised segmentation and genome annotation. *bioRxiv*. 2020;2020.01.30.926923.
62. Dixon JR, Selvaraj S, Yue F, Kim A, Li Y, Shen Y, et al. Topological domains in mammalian genomes identified by analysis of chromatin interactions. *Nature*. 2012;485(7398):376–380.
63. Mitra S, Zhong J, MacAlpine D, Hartemink AJ. RoboCOP: Jointly computing chromatin occupancy profiles for numerous factors from chromatin accessibility data. *bioRxiv*. 2020;2020.06.03.132001.
64. Rhee HS, Pugh BF. Comprehensive genome-wide protein-DNA interactions detected at single-nucleotide resolution. *Cell*. 2011;147(6):1408–1419.
65. He Q, Johnston J, Zeitlinger J. ChIP-nexus enables improved detection of *in vivo* transcription factor binding footprints. *Nature Biotechnology*. 2015;33(4):395.
66. Codogno M, Fissore L. Duration modelling in finite state automata for speech recognition and fast speaker adaptation. In: *ICASSP'87. IEEE International Conference on Acoustics, Speech, and Signal Processing*. vol. 12. IEEE; 1987. p. 1269–1272.
67. Fujimaki R, Morinaga S. Factorized Asymptotic Bayesian Inference for Mixture Modeling. In: Lawrence ND, Girolami M, editors. *Proceedings of the Fifteenth International Conference on Artificial Intelligence and Statistics*. vol. 22 of *Proceedings of Machine Learning Research*. La Palma, Canary Islands; 2012. p. 400–408.
68. Cowan N. The magical number 4 in short-term memory: A reconsideration of mental storage capacity. *Behavioral and Brain Sciences*. 2001;24(1):87–114.
69. Ernst J, Kheradpour P, Mikkelsen TS, Shores N, Ward LD, Epstein CB, et al. Mapping and analysis of chromatin state dynamics in nine human cell types. *Nature*. 2011;473(7345):43–49.

70. Roberts EG, Mendez M, Viner C, Karimzadeh M, Chan RC, Ancar R, et al. Semi-automated genome annotation using epigenomic data and Segway. *bioRxiv*. 2016;080382.
71. Church DM, Schneider VA, Graves T, Auger K, Cunningham F, Bouk N, et al. Modernizing reference genome assemblies. *PLoS Biol*. 2011;9(7):e1001091.
72. Frankish A, Diekhans M, Ferreira AM, Johnson R, Jungreis I, Loveland J, et al. GENCODE reference annotation for the human and mouse genomes. *Nucleic Acids Research*. 2019;47(D1):D766–D773.
73. Kent WJ, Sugnet CW, Furey TS, Roskin KM, Pringle TH, Zahler AM, et al. The human genome browser at UCSC. *Genome Research*. 2002;12(6):996–1006.
74. Zhou X, Maricque B, Xie M, Li D, Sundaram V, Martin EA, et al. The human epigenome browser at Washington University. *Nature Methods*. 2011;8(12):989–990.
75. Zerbino DR, Achuthan P, Akanni W, Amode MR, Barrell D, Bhai J, et al. Ensembl 2018. *Nucleic Acids Research*. 2017;46(D1):D754–D761.
76. Buske OJ, Hoffman MM, Ponts N, Le Roch KG, Noble WS. Exploratory analysis of genomic segmentations with Segtools. *BMC Bioinformatics*. 2011;12(1):415.
77. Ramírez F, Dünder F, Diehl S, Grüning BA, Manke T. deepTools: a flexible platform for exploring deep-sequencing data. *Nucleic Acids Research*. 2014;42(W1):W187–W191.
78. Quinlan AR, Hall IM. BEDTools: a flexible suite of utilities for comparing genomic features. *Bioinformatics*. 2010;26(6):841–842.
79. Kircher M, Witten DM, Jain P, O’Roak BJ, Cooper GM, Shendure J. A general framework for estimating the relative pathogenicity of human genetic variants. *Nature Genetics*. 2014;46(3):310–315.
80. Rao SS, Huntley MH, Durand NC, Stamenova EK, Bochkov ID, Robinson JT, et al. A 3D map of the human genome at kilobase resolution reveals principles of chromatin looping. *Cell*. 2014;159(7):1665–1680.
81. Zeng X, Li B, Welch R, Rojo C, Zheng Y, Dewey CN, et al. Perm-seq: mapping protein-DNA interactions in segmental duplication and highly repetitive regions of genomes with prior-enhanced read mapping. *PLoS Comput Biol*. 2015;11(10):e1004491.
82. Yen A, Kellis M. Systematic chromatin state comparison of epigenomes associated with diverse properties including sex and tissue type. *Nature Communications*. 2015;6:7973.
83. Ebert P, Schulz MH. Fast detection of differential chromatin domains with SCIDDO. *Bioinformatics*. 2020; p. btaa960.
84. Chen B, Kenari NS, Libbrecht MW. Continuous chromatin state feature annotation of the human epigenome. *bioRxiv*. 2018;473017.